BIOCHEMISTRY
including biophysical chemistry & molecular biology

Article

pubs.acs.org/biochemistry

Interactions of Soluble Guanylate Cyclase with a P-Site Inhibitor: Effects of Gaseous Heme Ligands, Azide, and Allosteric Activators on the Binding of 2′-Deoxy-3′-GMP

Ryu Makino,[†,*] Shinsuke Yazawa,[†] Hiroshi Hori,[‡] and Yoshitsugu Shiro[§,*]

[†]Department of Life Science, College of Science, Rikkyo University, Nishi-ikebukuro 3-34-1, Toshima-ku, Tokyo 171-8501, Japan
[‡]Center for Quantum Science and Technology under Extreme Conditions, Osaka University, Toyonaka, Osaka 560-8531, Japan
[§]RIKEN Harima Institute/Spring 8, 1-1-1 Kouto, Mikazuki-cho, Sayo-gun, Hyogo 679-5148, Japan

Supporting Information

ABSTRACT: Nitric oxide (NO) elicits a wide variety of physiological responses by binding to the heme in soluble guanylate cyclase (sGC) to stimulate cGMP production. Although nucleotides, such as ATP or GTP analogues, have been reported to regulate the signaling of NO binding from the heme site to the catalytic site, the other regulatory functions of nucleotides remain unexamined. Among the nucleotides tested, we found that 2′-d-3′-GMP acted as a potent noncompetitive inhibitor with respect to Mn-GTP, when the ferrous enzyme combined with NO, CO, or allosteric activator BAY 41-2272. 2′-d-3′-GMP also displayed nearly identical patterns of inhibition for the ferric enzyme, in which the binding of N_3^- or BAY 41-2272 significantly increased the inhibitory effects of the nucleotide. Equilibrium dialysis measurements using the CO-ligated enzyme in the presence of allosteric activators demonstrated that 2′-d-3′-GMP exclusively binds to the catalytic site of sGC. Furthermore, the affinity of 2′-d-3′-GMP for the enzyme was found to increase upon addition of foscarnet, an analogue of PP_i. These findings together with other kinetic results imply that 2′-d-3′-GMP acts as a P-site inhibitor probably by forming a dead-end complex, sGC−2′-d-3′-GMP−PP_i, in the catalytic reaction. The formation of the complex of the enzyme with 2′-d-3′-GMP does not seem to be associated with changes in the Fe−proximal His bond strength, because the CO coordination state or the redox potentials of the enzyme-heme complex are virtually unaffected.

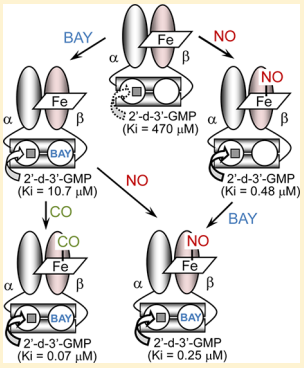

Soluble guanylate cyclase (sGC) is the best-characterized NO receptor involved in cell−cell signal transduction pathways associated with neuronal communication and vasodilation.[1−5] Mammalian sGC with a heterodimeric ($\alpha\beta$) structure binds a stoichiometric amount of heme via a weak bond between the heme iron and His105 of the β-subunit.[6−11] The binding of NO to the ferrous heme yields a five-coordinate NO−heme complex by cleaving the weak Fe−proximal His bond. The resultant five-coordinate NO−heme complex markedly stimulates the enzymatic production of cGMP.[7,11,12] The enzyme−heme complex also binds carbon monoxide (CO) with moderate stimulation of enzyme activity. Recent studies of the activation of sGC induced by NO suggest that the formation of the fully activated enzyme with the five-coordinate NO−heme complex occurs in two steps: a stable five-coordinate NO−heme species in a weakly active state converts to a highly active five-coordinate NO−heme species upon binding of an additional NO at an unknown site in the enzyme.[13−15] Nucleotides, including GTP, or allosteric activators, such as BAY 41-2272 [3-(4-amino-5-cyclopropylpyrimidin-2-yl)-1-(2-fluorobenzyl)-1*H*-pyrazolo-(3,4-*b*)pyridine] and YC-1 [3-(5′-hydroxymethyl-3′-furyl)-1-benzylindazole], accelerated the conversion to the highly active NO−heme species. Although these findings highlighted the significance of nucleotides or allosteric activators in the conversion, the detailed mechanism remained unresolved. To gain insight into the function of the nucleotide binding site(s), we have characterized the properties of the nucleotide binding site(s) using equilibrium dialysis.[16] Our results revealed that heterodimeric bovine sGC contains two classes of nucleotide binding sites: a catalytic site to bind the substrate (GTP) and another site that is pseudosymmetric to the catalytic site.[16] The latter site had been proposed to be a regulatory site that binds allosteric activator YC-1 or BAY 41-2272.[16,17]

To date, there is no crystal structure of NO-sensitive sGC. However, a detailed structure of the catalytic domain was deduced from the X-ray crystal structure of a eukaryotic sGC from *Chlamydomonas reinhardtii*.[18] The catalytic domain of this protein, which is located in the C-terminal segments, is 40% identical in amino acid sequence with that of the NO-sensitive mammalian sGC and contains the complete set of residues necessary for the catalysis. Comparison of the domain structure of the *C. reinhardtii* sGC with the known structures of adenylate cyclases confirmed the close similarity in architecture of catalytic site between these two enzymes. Although this study provided great insight into the functional analyses of mammalian sGCs, it was unable to analyze the interaction between the catalytic site

Received: March 30, 2012
Revised: October 29, 2012
Published: October 29, 2012

dx.doi.org/10.1021/bi3004044 | *Biochemistry* 2012, 51, 9277−9289

and the heme site because the structure lacked the heme-binding domain.

Previous inhibition studies of adenylate cyclase (AC) using adenosine and certain adenosine derivatives identified a binding site that strictly required an intact purine ring. Their locus of action has been designated a purine site (P-site).[19] These P-site inhibitors act noncompetitively or uncompetitively with respect to ATP, depending on the metal cofactor. The mode of inhibition is typically noncompetitive in the presence of Mn^{2+} and uncompetitive when Mg^{2+} is present. The sensitivity of the P-site inhibitors to the enzyme was potentiated when the enzyme was activated by a α-subunit of G-protein and/or forskolin. Furthermore, kinetic data for the reverse reaction revealed that a single P-site inhibitor molecule bound to the catalytic site after the addition of PP_i and was competitive with cAMP at the catalytic site of the enzyme.[20,21] On the basis of these kinetic studies, it is believed that P-site inhibitors form a dead-end complex (the enzyme−P-site inhibitor−PP_i) by occupying the site that previously accommodated the product cAMP in a reaction intermediate (AC−cAMP−PP_i). Indeed, X-ray structural and equilibrium dialysis studies revealed that the P-site inhibitor bound to the active site of AC together with PP_i.[20,22] As mentioned above, the activated forms of AC are more sensitive to P-site inhibition than the nonstimulated form of the enzyme. This is explained by the dead-end inhibition model.[19−21] Under the basal condition, the synthesis of cAMP is slow, and the release of PP_i from the enzyme is fast relative to the rate of cAMP synthesis. This results in the low concentration of the AC−PP_i complex. Upon activation by the α-subunit of G-protein and/or forskolin, cAMP is released from the enzyme more rapidly than the second product, PP_i. As a result, the enzyme−PP_i complex accumulates during the catalytic reaction and permits the binding of the P-site inhibitor with formation of the dead-end complex. We thought that P-site inhibitors might serve as valuable tools for the analysis of communication between the substrate domain and the heme domain in sGC. This is because a P-site inhibitor was expected to favorably bind to the catalytic site of the enzyme activated by CO or NO.

In this study, we obtained kinetic evidence supporting the idea that 2′-d-3′-GMP acts as potent P-site inhibitor for sGC. The apparent potency of the inhibitory action significantly increased when sGC was stimulated by the binding of heme-binding activators, such as NO or CO, and of allosteric activator BAY 41-2272. Equilibrium dialysis studies revealed that the affinity of 2′-d-3′-GMP for the resting ferrous sGC was extremely low but significantly increased when the ferrous sGC combined with CO in the presence of Mn^{2+}. Furthermore, foscarnet, an analogue of PP_i, augmented the affinity of 2′-d-3′-GMP for the CO-ligated enzyme with a stoichiometry of one binding site per heterodimer in the presence of BAY 41-2272 or YC-1. Our experimental findings are consistent with features of a P-site inhibitor revealed from studying adenylate cyclase. The binding characteristics of 2′-d-3′-GMP are unique and distinct from those of AMP-PNP, which acts as a competitive inhibitor by binding to the catalytic site of the resting enzyme. Similar inhibitory actions of 2′-d-3′-GMP were also observed for the ferric enzyme activated by N_3^-, which yielded a five-coordinate N_3^-−heme complex. Moreover, infrared spectroscopic and potentiometric titration studies indicate that the observed effect of 2′-d-3′-GMP on sGC activity is likely not mediated by disruption of the Fe−His bond of the heme.

EXPERIMENTAL PROCEDURES

Reagents. GTP, AMP-PNP, and 2′-d-3′-GMP were purchased from Sigma-Aldrich Japan (Tokyo, Japan). 2′-d-3′-GMP was further purified using a C18 HPLC column. YC-1 and BAY 41-2272 were purchased from ALEXIS (San Diego, CA). Other chemicals, purchased from Wako Chemicals Co. (Tokyo, Japan), were of the highest commercial grade.

Enzyme Purification. Bovine lung (5 kg) was minced and homogenized using a Waring blender in 15 L of 50 mM potassium phosphate buffer (pH 7.4) containing a mixture of protease inhibitors (1 mM phenylmethanesulfonyl fluoride, 1 mM benzamidine, and 1 mM ethylenediaminetetraacetic acid) and 55 mM β-mercaptoethanol.[11,16] The protocol for enzyme purification was essentially the same as that described previously,[16] except for the use of Mimetic Orange 1 affinity absorbent (Sigma-Aldrich, St. Louis, MO) in place of Cibacron Brilliant Red 3B-A affinity absorbent. The purified enzyme preparations supplemented with 5% glycerol and 5 mM DTT were stored in liquid nitrogen until they were used. The dibromodeuteroheme-substituted enzyme was prepared by the method described previously.[23]

Spectral Measurements. Optical absorption spectra at ambient temperature were recorded on a Perkin-Elmer Lambda 18 spectrophotometer. EPR spectra were measured on a Varian E-12 X-band spectrometer (Varian, Palo Alto, CA) with a 100 kHz field modulation.[11] The ferric enzyme employed for EPR measurements was prepared by adding a 2-fold excess of ferricyanide to the DTT-free ferrous enzyme, from which the residual ferricyanide was removed by passing through a Superdex 200HR (GE Healthcare, Tokyo, Japan) HPLC column. Infrared spectra were measured by a Perkin-Elmer Spectral One FTIR spectrophotometer (Perkin-Elmer, Tokyo, Japan) with a mercury−cadmium−telluride detector. The cell had CaF_2 windows with a light path length of 0.1 mm. The desired temperature of the cell was maintained by using a circulating water bath. The buffer consisted of 50 mM Hepes (pH 7.5) containing 50 mM NaCl and 5% (v/v) ethylene glycol.

Optical spectra at 77 K were recorded on an MPS-2450 spectrophotometer (Shimadzu, Kyoto, Japan) equipped with a homemade low-temperature attachment consisting of a liquid N_2 Dewar and twin cuvettes (light path, 1 mm) for sample and reference solutions, as reported previously.[24]

Oxidation−Reduction (Redox) Potential Measurements. The redox potentials were measured at 15 °C by a spectroelectrochemical titration apparatus, which was originally designed by us.[24] DTT included in the stored sGC solution was removed by the solution being passed through a Superdex 200HR column (GE Healthcare) to avoid undesired redox reactions. The following mediators were used: 2.5 μM 3-chlorophenolindophenol (+233 mV), 63 μM $Ru(NH_3)_6Cl_3$ (+120 mV), 13 μM pyocyanine (−34 mV), 13 μM 2,6-dichlorophenolindo-*o*-cresol (+180 mV), and 13 μM 2,6-dichloroindophenol (+215 mV) for redox titrations of sGC and 19 μM pyocyanine, 3 μM thionine (+64 mV), and 63 μM $Ru(NH_3)_6Cl_3$ for myoglobin. Other details are described in the corresponding figure legends.

Equilibrium Dialysis. The buffer used for equilibrium dialysis consisted of 50 mM Hepes (pH 7.5) containing 50 mM NaCl, 5% (v/v) ethylene glycol, and 3.5 mM Mg^{2+} or Mn^{2+}. DMF [6% (v/v)] was added to maintain the desired concentration of the poorly soluble YC-1 or BAY 41-2272. A five-cell equilibrium dialyzer (Spectrum Laboratories, Rancho

Dominguez, CA) was used for dialysis. In the experiments under CO, the samples were equilibrated with CO at 1 atm and then introduced into the chamber of equilibrium dialysis cells. Then, the headspace of the chamber was replaced with CO gas. The dialysis cells were shaken at a constant rate of 94 strokes per minute at 4 or 15 °C. After dialysis, YC-1 or nucleotides were quantified by HPLC analysis using a C18 or anion exchange column, respectively, at a constant flow rate of 1.0 mL/min. The amounts of enzyme-bound nucleotides or YC-1 were estimated from the difference in the concentration between the two half-cells, with and without enzyme. In experiments that aimed to assess the effects of activators (YC-1 and BAY 41-2272) or nucleotides (AMP-PNP, 2′-dADP, and cGMP) on the binding of 2′-d-3′-GMP, these compounds were included in both chambers of the dialysis cell. The dissociation constant (K_d) and the binding sites (B_{max}) for YC-1 and nucleotide binding were determined by nonlinear regression analyses using GraphPad Prism. Other experimental details either have been described previously[16] or are included in the figure legends of this study.

Activity Measurements. End point assays were conducted at 25 or 30 °C for the ferric and ferrous enzyme, respectively, in a water bath maintained with a Julabo F13 temperature controller. The assay mixture (200 μL) contained 5 mM $MgCl_2$ or $MnCl_2$, 50 mM NaCl, and 5% glycerol in 50 mM Hepes buffer (pH 7.5). For activity measurements of the ferrous enzyme, 5 mM DTT was added to the assay mixture described above. The assay for the CO-activated ferrous enzyme was conducted in septum-sealed vials, in which the headspace was filled with 1 atm of CO after the headspace had been flushed with CO gas for 1 min. In the assay using the ferric enzyme, DTT contained in the stored enzyme sample was removed with a Superdex 200HR column (GE Healthcare). The resultant DTT-free enzyme was added to the reaction mixture containing 35 μM ferricyanide as an oxidizing agent. When desired, 30 mM N_3^- was added to activate the ferric enzyme. Appropriate amounts of 2′-d-3′-GMP were included in the assay mixtures to analyze its inhibitory action for the ferric and ferrous enzyme. In every assay, reactions were started by the addition of enzyme. The reaction was terminated by the addition of 5 μL of 30% acetic acid. The amount of cGMP formed was quantified by analysis on a C18 HPLC column, as previously described.[11] The enzyme activities were expressed as the turnover number per heme. The kinetics was analyzed by linear regression analyses using GraphPad Prism. The data are presented with the standard error of the mean. Other details are described in the corresponding figure legends.

RESULTS

2′-d-3′-GMP as a P-Site Inhibitor. Several nucleotides, including 2′-d-3′-GMP, AMP-PNP, 2′-dADP, and GMP-CPP, were tested for their capacity to inhibit the cGMP production catalyzed by sGC in the absence and presence of NO. Among the nucleotides examined, 2′-d-3′-GMP strongly inhibited the NO-stimulated activity (in the presence of Mn^{2+}) in the submicromolar range, whereas the inhibitory effect was quite weak in the absence of NO. Such a remarkable increase in the inhibitory potency by NO was not observed for other nucleotides tested. The increase in the inhibitory potency in response to activation of the enzyme is a feature typical of a P-site inhibitor reported for adenylate cyclase. In this study, we analyzed the inhibitory mechanism focusing on the unique action of 2′-d-3′-GMP to obtain firm evidence that 2′-d-3′-GMP acted as a P-site inhibitor for soluble guanylate cyclase.

Inhibitory actions of 2′-d-3′-GMP for the ferrous sGC in the presence of Mn^{2+} are summarized in Figure 1. Inhibition of the

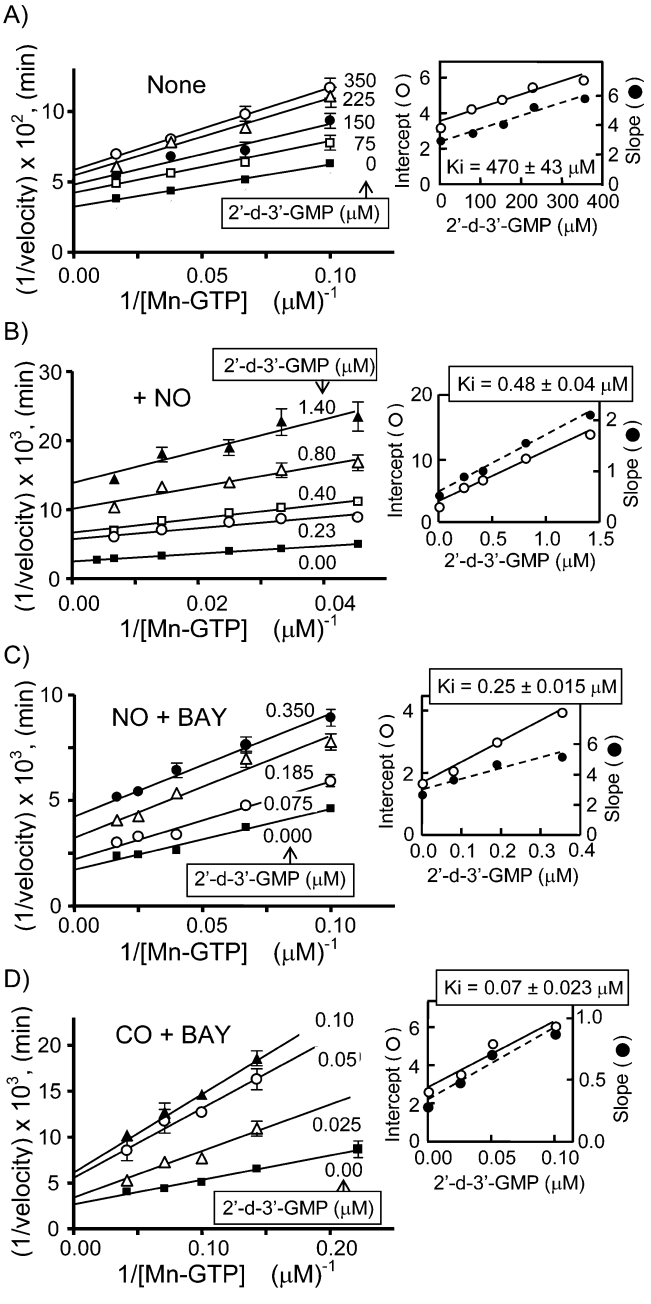

Figure 1. Noncompetitive inhibition by 2′-d-3′-GMP for the cyclase activity of the ferrous sGC. Assays were performed in the presence of 5 mM Mn^{2+}, 5 mM DTT, and an appropriate amount of GTP at 30 °C. The concentrations of 2′-d-3′-GMP included in the reaction mixture are given. The apparent K_i (inhibition constant) was determined by replots (in insets) of the intercept vs the corresponding concentrations of 2′-d-3′-GMP. Reactions were assayed (A) in the absence of activator and (B) in the presence of 50 μM SNAP as a NO generator. (C) BAY 41-2272 (35 μM) and SNAP (50 μM) were added to the reaction mixture. (D) Reactions were conducted in a mixture containing 35 μM BAY 41-2272 under 1 atm of CO. Data points were an average of three or four independent assays. The concentration of GTP was varied from 10 to 60 μM for panels A and C, from 22 to 250 μM for panel B, and from 4.5 to 25 μM for panel D. The final concentration of sGC was 3.4×10^{-8} M for panel A, 1.3×10^{-9} M for panel B, 3.1×10^{-9} M for panel C, and 4.5×10^{-9} M for panel D.

dx.doi.org/10.1021/bi3004044 | Biochemistry 2012, 51, 9277−9289

nonstimulated enzyme by 2′-d-3′-GMP was apparently noncompetitive with respect to Mn-GTP (Figure 1A). Similar noncompetitive kinetics with 2′-d-3′-GMP was observed in the presence of gaseous heme-binding activator NO, a combination of either NO or CO with BAY 41-2272 (Figure 1B−D), and BAY 41-2272 alone (data not shown). To identify the type of inhibition, the slope and the intercept of each Lineweaver−Burke plot were replotted against the corresponding concentration of 2′-d-3′-GMP (insets in Figure 1). As evident from the insets, the slopes and the intercepts are a linear function of 2′-d-3′-GMP concentration, suggesting that 2′-d-3′-GMP behaves as an essentially pure noncompetitive inhibitor in the absence and presence of the activator. The K_i values, which were calculated from the replots of intercepts versus inhibitor concentrations, decreased in the presence of Mn^{2+} in the following order: 470 ± 43 μM (no addition), 10.7 ± 1.6 μM (BAY), 0.48 ± 0.04 μM (NO), 0.25 ± 0.015 μM (NO and BAY), and 0.07 ± 0.023 μM (CO and BAY).

By contrast, 2′-d-3′-GMP exhibited apparently uncompetitive inhibition with respect to Mg-GTP in the absence and presence of NO, or in the presence of both CO and BAY 41-2272 (Figure S1 of the Supporting Information). As shown in the insets, the slopes were practically independent of 2′-d-3′-GMP concentration, while the intercepts were a linear function of 2′-d-3′-GMP concentration. These characteristics manifest that 2′-d-3′-GMP is an essentially pure uncompetitive inhibitor, despite the presence of an activator(s). The K_i values decreased in the presence of Mg^{2+} in the following order: 409 ± 35 μM (no addition), 2.5 ± 0.30 μM (NO), and 2.2 ± 0.16 μM (CO and BAY).

Soluble guanylate cyclase activated by gaseous heme-binding activator NO, BAY 41-2272, or a combination NO or CO with BAY was found to be more sensitive to 2′-d-3′-GMP than the nonstimulated enzyme, as judged from the apparent K_i values (Figure 1 and Figure S1 of the Supporting Information). These kinetic characteristics are reminiscent of the mode of action of P-site inhibitors reported for adenylate cyclase, because an activator such as forskolin potentiates the action of the P-site inhibitor. If 2′-d-3′-GMP acts as a P-site inhibitor in the sGC-catalyzed cyclase reaction, it is expected that 2′-d-3′-GMP and PP_i simultaneously bind to the catalytic site to form the dead-end complex (the enzyme−2′-d-3′-GMP−PP_i ternary complex). To address this issue, we examined the effects of PP_i on the cyclase reaction in the presence of Mg^{2+} and analyzed them with a Dixon plot. The Dixon plot of 1/velocity versus PP_i concentration in the presence of different fixed concentrations of 2′-d-3′-GMP yielded a series of lines without a common intersection at the vertical axis (Figure S1D of the Supporting Information), suggesting the simultaneous occupation of the same site by PP_i and 2′-d-3′-GMP. This supports a model yielding the dead-end complex (sGC−2′-d-3′-GMP−PP_i ternary complex). However, the kinetic efforts that test the possible formation of the dead-end complex in the presence of Mn^{2+} were unsuccessful, because of the limited solubility of the Mn−PP_i complex. As mentioned later, the formation of the enzyme−PP_i complex in the presence of Mn^{2+} was substantiated using foscarnet, a PP_i analogue.

Despite a similar core structure between substrate GTP and 2′-d-3′-GMP, 2′-d-3′-GMP acts noncompetitively or uncompetitively with respect to the substrate GTP in the presence of Mn^{2+} or Mg^{2+}, respectively. Such differential inhibition by a metal cofactor has also been noted for P-site-mediated inhibition of AC: Mn^{2+} usually yields noncompetitive kinetics and Mg^{2+} uncompetitive kinetics. This has been explained by assuming that Mn^{2+} induces conformational changes in the enzyme and permits binding of the inhibitor to the substrate-free enzyme.[20] As mentioned later, the direct binding assays by equilibrium dialysis revealed that the mechanism proposed for AC might be also valid for sGC.

The uncompetitive inhibition suggests that 2′-d-3′-GMP binds to the enzyme−substrate or −product complexes, while the noncompetitive inhibition implies that 2′-d-3′-GMP binds to the free enzyme in addition to the enzyme−substrate or −product complexes. Thus, the use of Mg^{2+} as a metal cofactor was expected to yield clearer findings because of the simpler pattern of inhibition. However, utilizing Mg^{2+} limited the direct measurements of 2′-d-3′-GMP binding because of its low affinity as described below. For this reason, the analyses of the inhibition mechanism by equilibrium dialysis were exclusively conducted in the presence of Mn^{2+}.

The P-site inhibition model for adenylate cyclase suggests that ATP and the P-site inhibitor bind with AC in a distinct conformation: ATP with resting AC and the inhibitor with the AC−PP_i complex.[20,21] Activation of AC by forskolin may lead to higher concentrations of the enzyme−PP_i complex under steady state conditions by altering the rate-limiting step and thus augments the potency of the P-site inhibitor. As shown in Figure 1, the inhibitory potency of 2′-d-3′-GMP for sGC increased upon addition of activator(s), supporting the P-site inhibition mechanism. Hence, it is likely that 2′-d-3′-GMP preferentially binds to sGC bound with an activator(s), rather than the nonstimulated sGC. To address this issue, we directly examined the requirements for the binding of 2′-d-3′-GMP using equilibrium dialysis (Figure 2). The amount of 2′-d-3′-GMP bound to the resting ferrous enzyme is considerably small relative to the amount bound to the CO-ligated form (the left column in Figure 2A). The affinity (K_d) is roughly estimated to be >800 μM by comparison to the affinity in the presence of BAY 41-2272 (Figure 2C). The addition of YC-1 in the absence of CO did not cause a substantial increase in the amount of bound 2′-d-3′-GMP (Figure 2A). By contrast, the binding of 2′-d-3′-GMP was readily detected by the addition of CO alone or the combined addition with BAY or YC-1 in the presence of Mn^{2+} (Figure 2A). These observations emphasize that 2′-d-3′-GMP preferentially binds to the CO-ligated form of the enzyme. Such a clear indication was not observed in the presence of Mg^{2+}, where only a modest level of binding was detected even in the presence of CO and BAY 41-2272 (inset in Figure 2A).

We attempted to identify the location for the binding of 2′-d-3′-GMP using AMP-PNP and 2′-dADP, both of which are known to bind to the catalytic site.[16] These two nucleotides effectively diminished the amount of bound 2′-d-3′-GMP (Figure 2A). cGMP also inhibited the binding of 2′-d-3′-GMP, presumably by competing for a common binding site. Analysis of the binding of 2′-d-3′-GMP to ferrous sGC in the presence of CO and Mn^{2+} identified a single binding site with a K_d of 87.8 ± 14.0 μM (Figure 2B). Further addition of either BAY 41-2272 or YC-1 increased the affinity of 2′-d-3′-GMP for CO-ligated sGC with a stoichiometry of one molecule of 2′-d-3′-GMP per heterodimer (K_d = 75.6 ± 17.6 μM in the presence of YC-1 and 58.8 ± 15.0 μM in the presence of BAY) (Figure 2B,C). The most straightforward way to rationalize these findings with the kinetic observations is to conclude that 2′-d-3′-GMP preferentially binds to the catalytic site on the stimulated enzyme by activators rather than the nonstimulated enzyme.

Noncompetitive inhibition observed in the presence of Mn^{2+} implies that 2′-d-3′-GMP binds to the product (PP_i) complex as

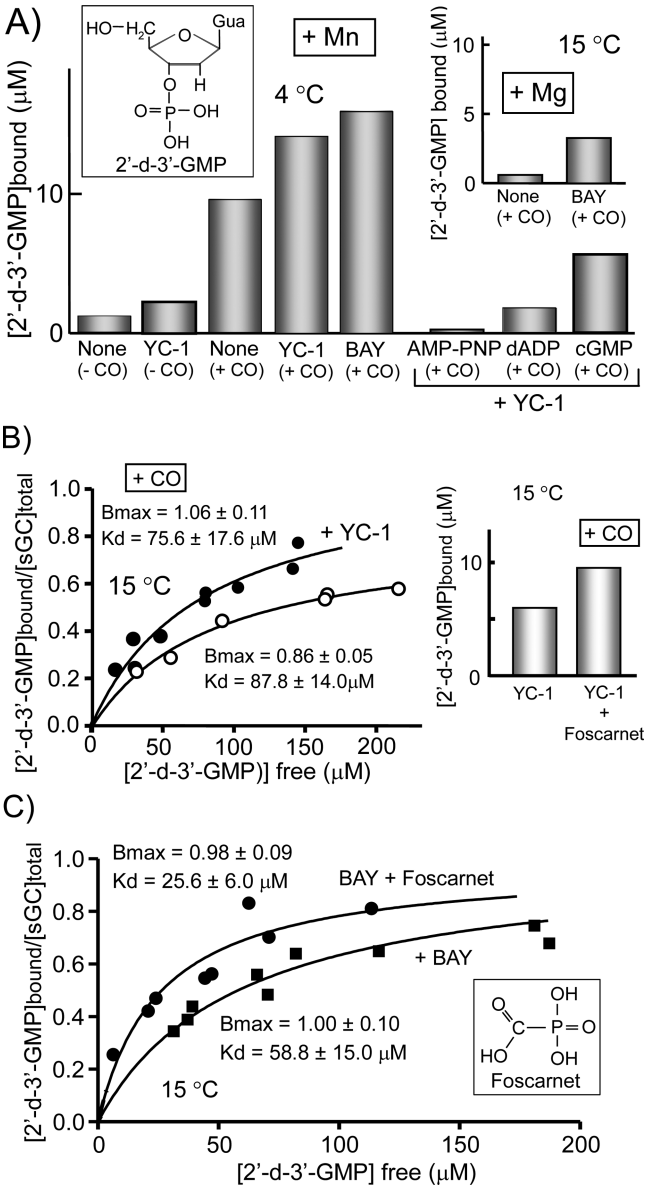

Figure 2. Binding of 2′-d-3′-GMP to the ferrous enzyme by equilibrium dialysis in the presence and absence of CO. (A) Binding of 400 μM 2′-d-3′-GMP to 20 μM ferrous sGC was measured in the absence and presence of CO at 4 °C. Concentrations were as follows: 100 μM YC-1, 80 μM BAY 41-2272, 110 μM AMP-PNP, 425 μM dADP, and 4.5 mM cGMP. In these experiments, 3.5 mM Mn^{2+} was included in the mixture. In the inset, reactions of sGC (17 μM) with 2′-d-3′-GMP (360 μM) were assessed in the presence of CO and Mg^{2+} at 15 °C. (B) Reaction mixtures contained 20−380 μM 2′-d-3′-GMP and 14.5−18.5 μM ferrous enzyme in the absence (○) and presence (●) of 100 μM YC-1 at 15 °C. The inset shows the effect of YC-1 (100 μM) and/or foscarnet (480 μM) on the reaction between 360 μM 2′-d-3′-GMP and 16 μM sGC under a CO atmosphere at 15 °C. (C) Reaction mixtures contained 20−380 μM 2′-d-3′-GMP and 14.5−18.5 μM ferrous enzyme in the presence of 80 μM BAY 41-2272 (■) and in the presence of 80 μM BAY and 480 μM foscarnet (●) under a CO atmosphere at 15 °C. The experiments for panels B and C were conducted in the presence 3.5 mM Mn^{2+}. The best fit curves obtained by nonlinear regression analyses are illustrated as solid lines. Structures of 2′-d-3′-GMP and foscarnet are given in panels A and C, respectively.

well as the enzyme in the resting state (regardless of whether the activator exists). We thus tested the capacity of PP_i to support the binding of 2′-d-3′-GMP to CO-sGC by equilibrium dialysis. However, the experiments in the presence of Mn^{2+} failed because of the limited solubility of the Mn−PP_i complex. Foscarnet, an analogue of PP_i, exhibited higher solubility in the presence of Mn^{2+} than PP_i and acted as a competitive inhibitor with respect to Mn-GTP (data not shown). This strongly suggested that foscarnet binds to a site accommodating PP_i in the presence of Mg^{2+}. Direct binding experiments for examining the action of foscarnet are summarized in panels B (inset) and C of Figure 2. These experiments, which were conducted in the presence of CO and BAY 41-2272 or YC-1, indicated that foscarnet does not compete with but rather augments the binding of 2′-d-3′-GMP without affecting the binding stoichiometry. Consequently, 2′-d-3′-GMP is capable of binding to the CO-bound enzyme with or without foscarnet in the presence of Mn^{2+}. This result accounts for the noncompetitive kinetics in the presence of Mn^{2+} (i.e., the formation of the enzyme−2′-d-3′-GMP−PP_i complex in addition to the enzyme−2′-d-3′-GMP complex).

The results in Figure 2A demonstrate that the binding of 2′-d-3′-GMP markedly depends on the presence of CO. This suggests that 2′-d-3′-GMP can discriminate subtle structural change in the catalytic site after binding CO. We thought that this unique characteristic is specific to the P-site inhibitor, not the competitive inhibitor, because the competitive inhibitor binds solely to the enzyme in the resting state. To substantiate and evaluate the possibility, we examined the binding characteristics of AMP-PNP that behaved as a pure competitive inhibitor with respect to Mn-GTP[16] in the presence and absence of CO and compared them with those of 2′-d-3′-GMP. In this work, the direct binding assays were conducted in the presence of Ca^{2+} as a metal cofactor, to avoid the conversion of AMP-PNP to cAMP catalyzed by the CO-activated form of sGC in the presence of Mn^{2+}. To the best of our knowledge, Ca^{2+} is a potent inhibitor for the guanylate cyclase reaction. Nonetheless, the replacement of Mn^{2+} with Ca^{2+} merely impaired the affinities of AMP-PNP, GMP-CPP, and 2′-dADP for the ferrous enzyme without changes in the binding stoichiometry of these nucleotides.[16] Accordingly, it is suggested that Ca^{2+} contributes to the recognition of the nucleotide through mechanisms analogous to that of Mn^{2+} or Mg^{2+}, although Ca^{2+} cannot support catalysis. Indeed, in an isoform of adenylate cyclase, Ca^{2+} occupied the high-affinity metal site and inhibited the activity by stabilizing the inactive (open) conformation in both ATP- and PP_i-bound states.[25] However, the detailed roles of the metal cofactor for nucleotide recognition and catalysis remain unresolved for NO-sensitive sGC. As shown in Figure S2 of the Supporting Information, AMP-PNP bound to the resting ferrous enzyme with a K_d of 7.4 ± 1.2 μM in the presence of Ca^{2+}. This agrees with the previous value obtained under comparable conditions.[16] The ligation of CO at the enzyme−heme complex has essentially no effect on the binding of AMP-PNP (Figure S2 of the Supporting Information). Furthermore, foscarnet prevents the binding of AMP-PNP to the catalytic site (Figure S2 of the Supporting Information). These binding characteristics are distinct from those of 2′-d-3′-GMP and strongly suggest that AMP-PNP is unable to discriminate the conformational difference before and after the binding of CO to sGC. These results taken together again emphasize that 2′-d-3′-GMP can bind to the CO-ligated enzyme by discriminating subtle conformational changes in the catalytic site after the binding of CO to sGC.

Interaction of the Catalytic Site with the Allosteric Activator Binding Site. Panels A and B of Figure 2 demonstrate that 2′-d-3′-GMP and allosteric activators, such as

dx.doi.org/10.1021/bi3004044 | Biochemistry 2012, 51, 9277−9289

BAY 41-2272 and YC-1, bind to distinct sites on the CO-ligated enzyme. This finding suggests at least two possible mechanisms, depending on whether the two different sites interact with each other or bind each effector independently. To distinguish between these possibilities, we assessed the effects of 2′-d-3′-GMP on the binding of YC-1 by equilibrium dialysis. As shown in Figure 3, the affinity of YC-1 for CO-sGC was 119 ± 29.8 or 73.4 ± 14.5 μM at 15 or 25 °C, respectively. In the presence of excess 2′-d-3′-GMP, the affinity of YC-1 increased to ~25 μM (26.7 ± 2.4 μM at 15 °C and 24.3 ± 3.8 μM at 25 °C) (Figure 3A,B). This observation, together with the results shown in panels A and B of Figure 2, which show a significant increase in the level of 2′-d-3′-GMP binding by the addition of YC-1 or BAY 41-2272, may be a direct indication of cooperative intramolecular interaction between the catalytic site and the allosteric activator site. Taken together, these results show that the binding of 2′-d-3′-GMP to the catalytic site has an effect on the properties of the YC-1 binding site and vice versa, in addition to the communication between the heme site and the catalytic site.

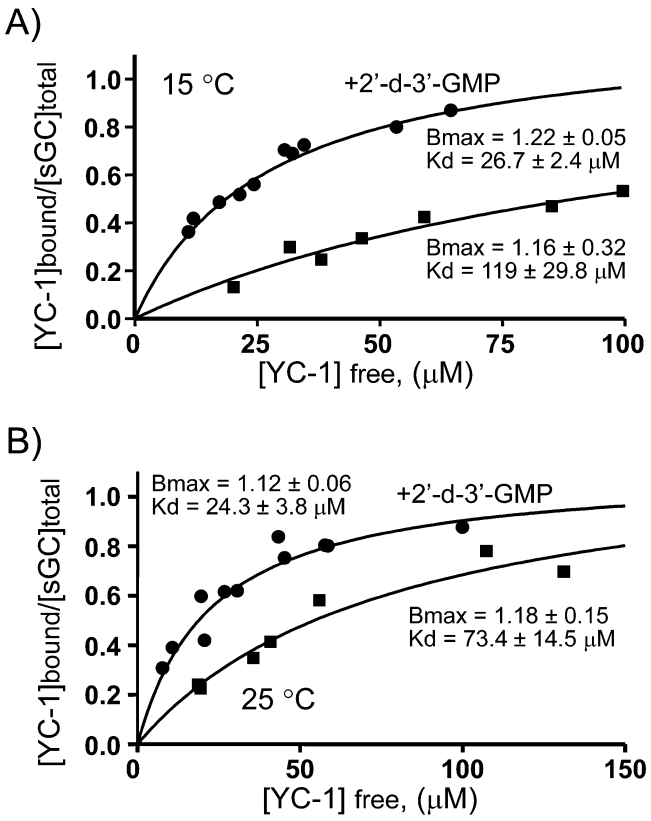

Figure 3. Effects of 2′-d-3′-GMP on the binding of YC-1 in the presence of CO. (A) YC-1 binding in the presence of CO and 3.5 mM Mn^{2+} (■) and in the presence of CO, 3.5 mM Mn^{2+}, and 500 μM 2′-d-3′-GMP (●) at 15 °C. (B) YC-1 binding in the presence of CO and 3.5 mM Mn^{2+} (■) and in the presence of CO, 3.5 mM Mn^{2+}, and 500 μM 2′-d-3′-GMP (●) at 25 °C. In these experiments, reaction mixtures contained 34−210 μM YC-1 and 13.5−15.8 μM ferrous enzyme. The best fit curves obtained by nonlinear regression analyses are illustrated as solid lines.

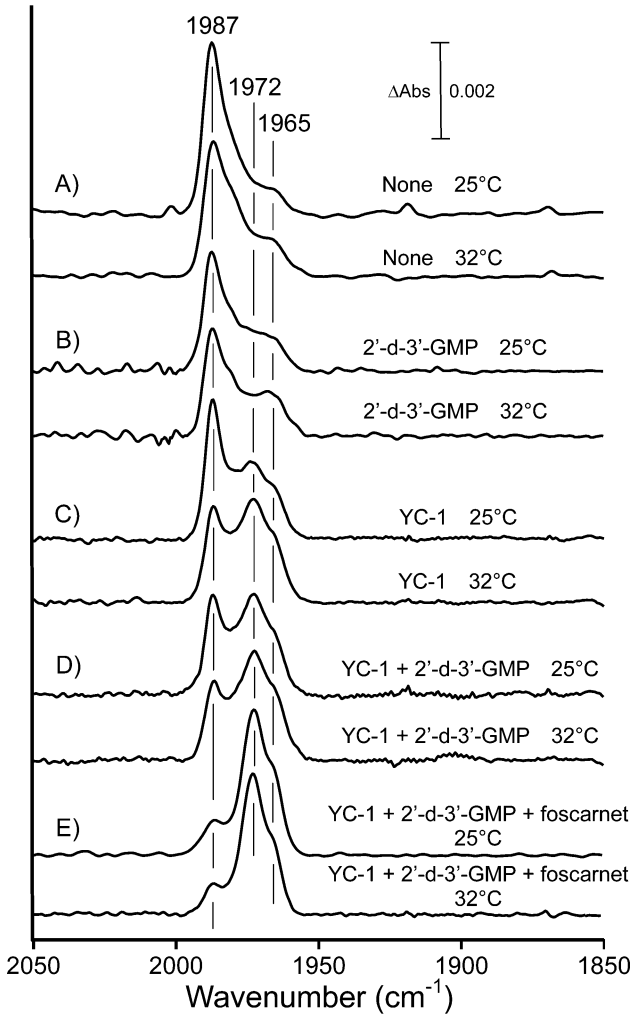

Figure 4. Fourier transform infrared spectra of the CO complex measured in the presence of 5.0 mM Mn^{2+} and 5.0 mM DTT at 25 and 32 °C. (A) Infrared νC−O stretching with no other addition. (B) νC−O stretching in the presence of 480 μM 2′-d-3′-GMP. (C) νC−O stretching in the presence of 200 μM YC-1. (D) Effect of 500 μM 2′-d-3′-GMP on the νC−O stretching in the presence of 200 μM YC-1. (E) Effect of the combined addition of 500 μM 2′-d-3′-GMP and 690 μM foscarnet on the νC−O stretching in the presence of 200 μM YC-1. The concentrations of sGC used for these experiments were 164 μM as heme.

The enhancement of the affinity of YC-1 for 2′-d-3′-GMP was further corroborated by infrared measurements, which are summarized in Figure 4. The ferrous sGC in the five-coordinate state yielded two forms of six-coordinate, low-spin CO adducts upon exposure to CO (Figure 4A): the dominant form of the CO adduct exhibited a sharp major C−O stretching (νC−O) band at 1987 cm^{-1}, while a minor component was observed around 1970 cm^{-1}. The addition of 2′-d-3′-GMP caused a minor change in νC−O (Figure 4B). A similar change has been also noted in the presence of other nucleotides such as 2′-dADP and AMP-PNP.[16] Comparison of the infrared spectra (Figure 4A,C) shows that the binding of YC-1 shifted infrared C−O stretching bands to 1972 and 1965 cm^{-1} with a concomitant decrease in the magnitude of the sharp 1987 cm^{-1} band. Therefore, the C−O stretching bands at 1972 and 1965 cm^{-1} are useful as spectroscopic probes for the binding of YC-1.[23] As has been already reported, the νC−O band of the CO−enzyme complex combined with YC-1 or BAY 41-2272 is composed of a mixture of five- and six-coordinate CO−heme complexes: the primary νC−O band at 1972 cm^{-1} is assigned to the six-coordinate CO−heme complex and the minor 1965 cm^{-1} band to the five-coordinate CO−heme complex.[23,26] As shown in Figure 4C, the band intensities of the YC-1-bound form of the CO−sGC complex at 1972 and 1965 cm^{-1} increased

dx.doi.org/10.1021/bi3004044 | Biochemistry 2012, 51, 9277−9289

when the temperature was elevated. This temperature-dependent change was fully reversible (data not shown). The temperature-dependent analyses of the νC−O bands demonstrated an increase in the affinity of YC-1 with an increase in temperature. Analogous reversible temperature-dependent increases in the magnitudes of the νC−O bands with an increase in temperature were also noted for the CO complex with BAY 41-2272 (Figure S3 of the Supporting Information). These observations confirm the findings from the direct binding studies, which showed an increase in the affinity of YC-1 with an increase in temperature (Figure 3). Additionally, it is clear that the addition of 2′-d-3′-GMP alone or the combined addition of 2′-d-3′-GMP with foscarnet increases the level of the YC-1- or BAY 41-2272-bound form (Figure 4D,E and Figure S3 of the Supporting Information). The 2′-d-3′-GMP-dependent increase in the level of the YC-1-bound form agrees with the dialysis studies, which show that 2′-d-3′-GMP enhances YC-1 affinity (Figure 3).

As mentioned above, the CO−enzyme complex with YC-1 or BAY 41-2272 is composed of a mixture of five- and six-coordinate CO−heme complexes. The formation of the five-coordinate CO−heme complex is the first example to be described from among hemoproteins and absolutely requires the presence of YC-1 or BAY 41-2272. Although the exact mechanism remains unknown, there is no doubt that the formation of the five-coordinate CO−heme complex may be associated with the weak Fe−proximal His bond. To discern whether 2′-d-3′-GMP cleaves the Fe−proximal His bond, we analyzed the νC−O band focusing on the formation of the five-coordinate CO−heme complex. This is crucial in understanding the action of 2′-d-3′-GMP. When the five-coordinate/six-coordinate CO−heme ratio was compared in the absence and presence of 2′-d-3′-GMP, it was noted that the ratio slightly decreased at 25 °C and essentially remained unchanged at 32 °C (compare panels C and D of Figure 4). Thus, the binding of 2′-d-3′-GMP to the CO−sGC complex in the presence of YC-1 is not likely to facilitate cleavage of the Fe−proximal His bond. The effect of 2′-d-3′-GMP was further investigated in the presence of foscarnet (Figure 4E). Under the experimental conditions, foscarnet augmented the production of the YC-1-bound form of the CO−sGC complex by increasing the affinity of 2′-d-3′-GMP, as mentioned already. Despite a remarkable increase in the YC-1-bound form upon combined addition of 2′-d-3′-GMP and foscarnet, the five-coordinate/six-coordinate CO−heme ratio exhibits only a slight decrease when compared with that in the presence of YC-1 alone at the same temperature (compare panels C and E of Figure 4). A more clear-cut result was obtained in the case of the BAY 41-2272-bound form (Figure S3 of the Supporting Information). In this case, the νC−O stretch at 1964 cm^{-1}, which can be assigned to the five-coordinate CO−heme complex,[26] is more intense relative to that in the presence of YC-1. The infrared C−O stretching bands of the BAY-bound form in the absence of 2′-d-3′-GMP can be superimposed on those in which 2′-d-3′-GMP was supplemented with BAY 41-2272, when the experiment was conducted at the same temperature. Taken together, these findings suggest that 2′-d-3′-GMP does not induce significant formation of the five-coordinate CO−heme complex by cleaving the Fe−proximal His105 bond.

Effects of 2′-d-3′-GMP on the N_3^- Binding of the Ferric Enzyme. We have previously reported that N_3^- is capable of stimulating the production of cGMP by the ferric enzyme.[11] The activity of the N_3^--stimulated ferric enzyme, expressed as the maximal cGMP production per enzyme−heme complex, was 560 or 125 min^{-1} in the presence of Mg-GTP or Mn-GTP, respectively, at 30 °C. Each activity is approximately 30% of that of the NO-stimulated ferrous enzyme in the presence of the corresponding metal (1610 and 405 min^{-1} in the presence of Mg-GTP and Mn-GTP, respectively, at 30 °C) (data not shown). In this study, we analyzed the inhibitory effect of 2′-d-3′-GMP on the N_3^--stimulated activity. As shown in Figure 5 and Figure S4

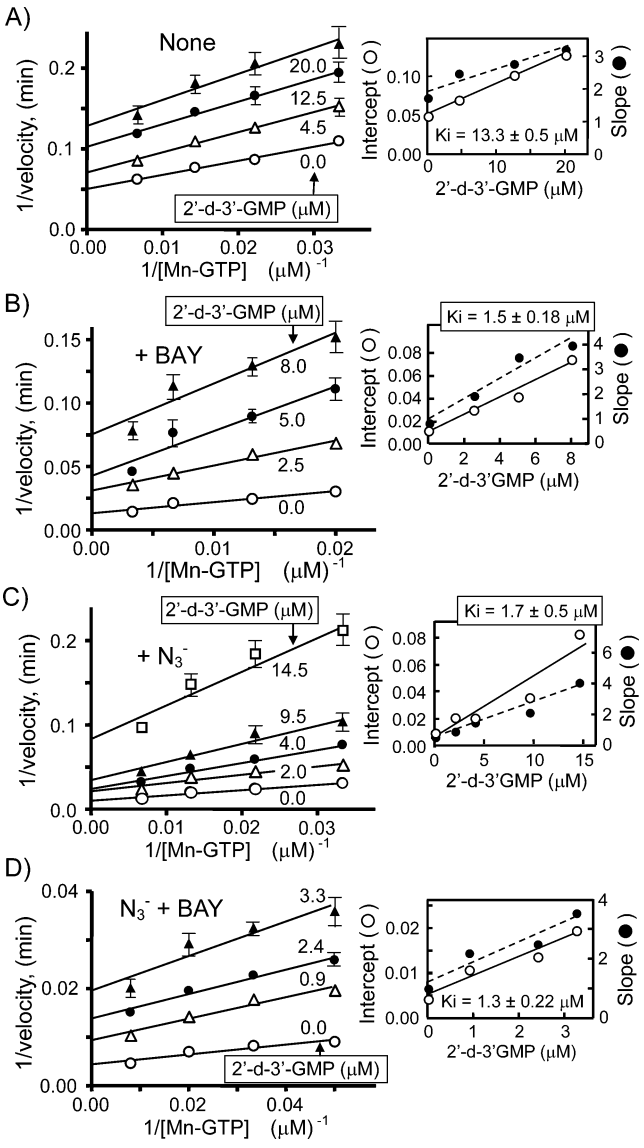

Figure 5. Noncompetitive inhibition by 2′-d-3′-GMP for the ferric sGC-supported cyclase activity. Assays were performed in the presence of 5 mM Mn^{2+} and 35 μM ferricyanide at 25 °C. The concentration of GTP was varied from 20 to 300 μM. The amounts of 2′-d-3′-GMP included in the reaction mixture are indicated in the figures. Analyses were performed by Lineweaver−Burke plot. Replots (insets) of the intercept vs the corresponding concentrations of 2′-d-3′-GMP were used to determine the apparent K_i (inhibition constant) similar to that described in Figure 1. Reaction mixtures were assayed (A) with no other addition and (B) in the presence of 35 μM BAY 41-2272. Reaction mixtures were analyzed (C) in the presence of 30 mM N_3^- or (D) in the presence of 35 μM BAY 41-2272 and 30 mM N_3^-. Data points were an average of four independent assays. The enzyme concentration used for each assay was 9.3×10^{-8} M for panel A, 2.4×10^{-8} M for panel B, 3.9×10^{-8} M for panel C, and 1.2×10^{-8} M for panel D.

dx.doi.org/10.1021/bi3004044 | Biochemistry 2012, 51, 9277−9289

of the Supporting Information, 2′-d-3′-GMP appears to noncompetitively inhibit the production of cGMP by the nonstimulated or stimulated enzyme in the presence of either Mg^{2+} or Mn^{2+}. The inhibitory action in the presence of Mn^{2+} was more potent for the ferric enzyme activated by BAY, N_3^-, or a combination of both species with a K_i of ~1.5 μM (K_d = 1.5 ± 0.18 μM in the presence of BAY, 1.7 ± 0.50 μM in the presence of N_3^-, and 1.3 ± 0.22 μM in the presence of N_3^- and BAY) (Figure 5B–D), while the nonstimulated ferric enzyme was less reactive for 2′-d-3′-GMP (K_i = 13.3 ± 0.5 μM) (Figure 5A). A similar but more clear-cut effect of allosteric activator BAY 41-2272 was evident using Mg^{2+} as the metal cofactor (K_i = 186 ± 39 μM in the presence of N_3^- and 15.0 ± 2.8 μM in the presence of N_3^- and BAY) (Figure S4 of the Supporting Information).

The infrared C–O stretching in Figure 4B (compared with Figure 4A) exhibited a slight increase in the intensity of the band at ~1967 cm^{-1} upon addition of 2′-d-3′-GMP, suggesting that this nucleotide modulates the reactivity of the heme. Indeed, 2′-d-3′-GMP had an effect on the binding of N_3^-, as estimated by spectrophotometric titrations (Figure 6). The ferric enzyme

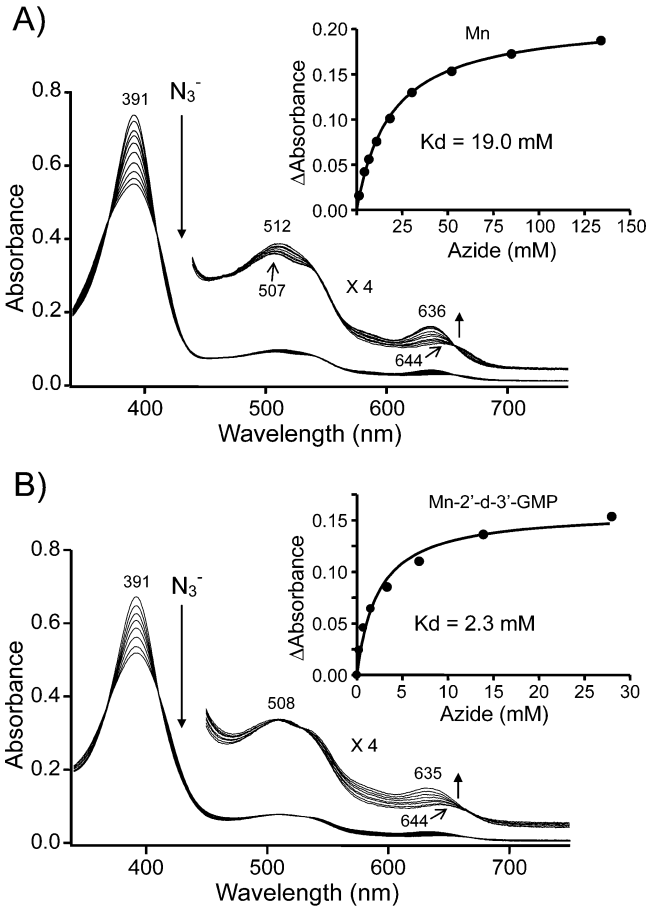

Figure 6. Optical spectrophotometric titration of N_3^- with ferric native sGC at 15 °C. The binding of N_3^- to native sGC was measured in the presence of 2.1 mM Mn^{2+} (A) or in the presence of 2.1 mM Mn^{2+} and 1 mM 2′-d-3′-GMP (B). The affinities of N_3^- (K_d) were estimated by nonlinear regression analysis. The buffer consisted of 40 mM Hepes buffer (pH 7.5) containing 5% ethylene glycol, 50 mM NaCl, and 85 μM ferricyanide.

exhibited the spectrum that can be assigned to the five-coordinate high-spin state with a Soret band at 391 nm as well as 512 and 644 nm bands (Figure 6A). The successive addition of N_3^- markedly reduced the Soret band intensity with the appearance of a new band at 636 nm. The conversion occurs with a set of isosbestic points. Analogous spectral changes were also observed in the presence of 2′-d-3′-GMP (Figure 6B). As shown, the inclusion of 2′-d-3′-GMP increased the affinity of N_3^- for the enzyme from 19 to 2.3 mM, indicating that the ferric heme in the nucleotide-bound enzyme had a high reactivity for N_3^-, while the heme in the resting enzyme was less reactive. Further addition of foscarnet slightly increased the affinity (1.5 mM) of the ferric enzyme for N_3^- (data not shown). This is a significant finding because it supports the proposal that 2′-d-3′-GMP is capable of binding to the catalytic site together with foscarnet and thus increasing the reactivity of the ferric heme for N_3^-.

The N_3^--induced spectral changes are unique. This is because the N_3^- complex of other hemoproteins generally exhibits clear split bands at ~540 and ~580 nm in the visible region, a red shift of the Soret band to ~420 nm, and a marked reduction in the intensity of the high-spin band at ~640 nm (indicating the formation of a six-coordinate low-spin N_3^-–heme state). These findings for sGC suggest that the N_3^-–heme complex of sGC is not in a six-coordinate low-spin state. To address the question of whether the anomalous spectral changes arise from the binding of N_3^- to a site other than the heme, we attempted to solve this issue by infrared spectroscopy. The N_3^- alone exhibited broad N_3^- stretching (νN=N=N$^-$) at 2049 cm^{-1} (trace a in Figure 7A). When 0.5 mM N_3^- was allowed to react with 2.5 mM ferric myoglobin, two νN=N=N$^-$ bands at 2045 and 2023 cm^{-1} appeared with a complete loss of the 2049 cm^{-1} νN=N=N$^-$ band of free N_3^- (trace b in Figure 7A). The band at 2045 cm^{-1} has been assigned to the six-coordinate high-spin N_3^-–heme complex and the band at 2023 cm^{-1} to the six-coordinate low-spin N_3^-–heme complex.[27] The 0.5 mM N_3^- solution containing 0.5 mM sGC displayed the νN=N=N$^-$ band at 2048 cm^{-1} (trace d in Figure 7A). This infrared spectrum seemed to be indistinguishable from that of free N_3^- (trace a in Figure 7A) but slightly differed in wavelength and bandwidth from those of free N_3^-. Indeed, the difference spectrum between trace a and trace d demonstrated the formation of a small amount of the N_3^-–heme complex (inset in Figure 7A). This slight difference reflects the low affinity of N_3^- for sGC. Next, we have tried to obtain a clear indication of N_3^- binding at the heme site using a dibromodeuteroheme-substituted enzyme. This is because the heme-substituted enzyme has an affinity for N_3^- (K_d = 0.63 mM in the presence of 2′-d-3′-GMP) that is higher than that of the native sGC in the presence of 2′-d-3′-GMP (Figure S5 of the Supporting Information), and the heme substitution does not cause significant changes in the νN=N=N$^-$ band as shown for myoglobin (traces b and c in Figure 7A). The νN=N=N$^-$ band of the heme-substituted sGC was located at 2038 cm^{-1} (trace e in Figure 7A). The significant shift of the νN=N=N$^-$ band provides evidence of ligation of N_3^- at the heme site. This supports the previous notion that cyanide markedly inhibited the N_3^--mediated cyclase activity by competing at the heme site with N_3^-.[11]

The coordination and spin states of the N_3^- complex were analyzed by EPR and low-temperature optical spectroscopic methods in the absence and presence of nucleotides (Figure 7B and Figure S6 of the Supporting Information). As has been reported previously,[11] the resting ferric enzyme exhibited a pure high-spin EPR signal with rhombic symmetry: g_1 = 6.62, g_2 = 5.36, and g_3 = 1.98 at 5 K (trace a in Figure 7B) or 15 K.[11] The low-temperature optical spectrum at 77 K also supports the

dx.doi.org/10.1021/bi3004044 | Biochemistry 2012, 51, 9277–9289

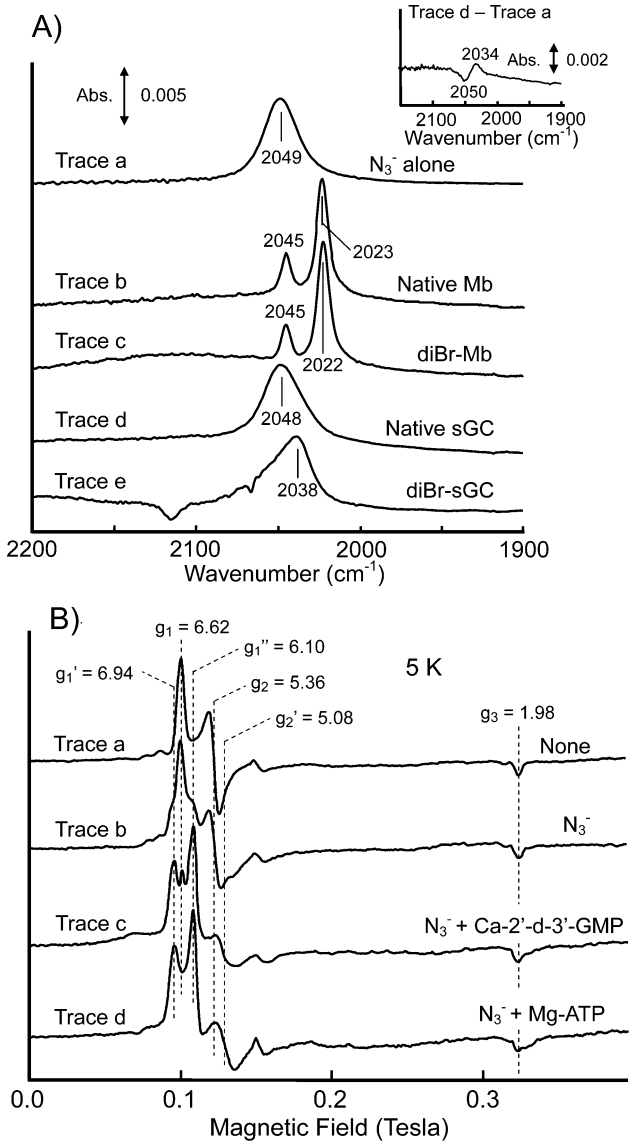

Figure 7. Spectroscopic analyses of the coordination and spin states of the N_3^- complex. (A) Trace a denotes the νN=N=N$^-$ stretching of N_3^- alone (0.5 mM). Traces b–d show the νN=N=N$^-$ stretching for the N_3^- complex of ferric sperm whale myoglobin (Mb) and sGC, together with their dibromodeuteroheme (diBr)-substituted proteins. The N_3^- complexes were formed by adding 0.5 mM N_3^- to 2.5 mM native and diBr-substituted myoglobins or to 0.5 mM native and diBr-substituted sGCs. In the experiment used to create trace e, 1 mM 2′-d-3′-GMP and 2.1 mM Mn^{2+} were further added to the mixture. The inset shows the difference spectrum between the sGC–N_3^- complex (trace d) and N_3^- alone (trace a). Data were collected at 15 °C. (B) The EPR spectrum measured at 5 K with no other addition is illustrated as trace a. Trace b shows the EPR spectrum in the presence of 50 mM N_3^- at 5 K. Traces c and d are the spectra obtained by addition of 0.5 mM Ca-2′-d-3′-GMP and 1 mM Mg-ATP, respectively, in the presence of 50 mM N_3^- at 5 K. These nucleotide complexes were produced in the presence of 2 mM Ca^{2+} or Mg^{2+}. The buffer consisted of 40 mM TEA buffer (pH 7.5) containing 50 mM NaCl and 5% ethylene glycol.

interpretation described above (trace a in Figure S6A of the Supporting Information). The binding of N_3^- produced two more high-spin species characterized by $g_1' = 6.94$ and $g_1'' = 6.10$ EPR signals (trace b in Figure 7B). In the subsequent EPR experiments, the effects of the nucleotide on the spin and coordination states of the heme were examined in the presence of Mg^{2+} or Ca^{2+}: Mg^{2+} or Ca^{2+} was used instead of Mn^{2+} to avoid the overlapping of intense EPR signals of Mn^{2+} in the $g = 2$ region. The addition of Ca-2′-d-3′-GMP or Mg-ATP increased the level of the high-spin species with the $g_1' = 6.94$ signal as well as the $g_1'' = 6.10$ signal (traces c and d in Figure 7B), indicating that these nucleotides significantly increased the affinity of N_3^-. The formation of these two high-spin species ($g_1' = 6.94$, and $g_1'' = 6.10$) is also detected upon addition of substrate analogue Mg-GMP-PNP (data not shown). It should be noted that these sGC–nucleotide complexes do not show significant low-spin EPR signals in the magnetic field around 0.2–0.3 T. These results are consistent with those obtained by low-temperature optical spectroscopy at 77 K, where the N_3^-–heme complex in the presence of Ca-2′-d-3′-GMP or Mg-ATP is practically in a high-spin state as underlined by the intense band at ~630 nm (traces c and d in Figure S6 of the Supporting Information). In addition, the replacement of Ca^{2+} with Mn^{2+} in the presence of 2′-d-3′GMP (or replacement of Mg^{2+} with Mn^{2+} in the presence of ATP) caused no detectable changes in the optical spectra at 77 K (data not shown). Furthermore, the low-spin EPR signals were virtually undetectable in the presence of Mg-ATP even when the measurements were performed at 15 K (Figure S6B of the Supporting Information). To the best of our knowledge, the appearance of the intense high-spin band around 630 nm associated with N_3^- binding is specific to sGC. Our results strongly suggested that N_3^- exclusively produces a five-coordinate high-spin heme by breaking the Fe–proximal His105 bond.

Effects of 2′-d-3′-GMP and BAY 41-2272 on the Redox Potential of the Heme. To investigate whether the binding of 2′-d-3′-GMP modulates the Fe–proximal His bond, we examined the redox potentials of the heme iron of sGC by spectroelectrochemical titrations. Experiments were conducted in the absence and presence of BAY 41-2272, or with a combination of 2′-d-3′-GMP, BAY 41-2272, and foscarnet (Figure 8). Spectroelectrochemical titrations under these conditions indicated that the redox reactions were fully reversible as confirmed by fitting the data points obtained in the course of reductive and oxidative titrations to a Nernst equation with $n = 1$ (Figure 8). Under these experimental conditions, the midpoint potential of the enzyme–heme complex in sGC was +202 mV versus the normal hydrogen electrode (Figure 8A). This value was slightly higher than our previous data measured at 20 °C (+187 mV).[24] The midpoint potential determined in this experiment was slightly low relative to the value for the heme domain of sGC from *Manduca sexta*, +234 mV at pH 7.4.[28] The midpoint potential of sGC was unaffected by the binding of BAY 41-2272 in the presence of Mg^{2+} (Figure 8B) and in the presence of foscarnet and Mn^{2+} (data not shown). Additionally, the binding of Ca-GMP-PNP to the catalytic site also has no effect on the midpoint potential of the enzymatic heme (+200 mV) (data not shown).

We attempted to assess the effect of 2′-d-3′-GMP on the Fe–His bond by redox potential measurements in the absence of CO. However, 2′-d-3′-GMP exhibited no significant affinity for the unliganded ferrous enzyme under the conditions we have tested previously for its binding. Using the equilibrium dialysis, we assessed whether foscarnet has the capacity to form the complex between 2′-d-3′-GMP and the ferrous enzyme. When excess foscarnet was supplemented with BAY 41-2272 in the presence of Mn^{2+}, it is confirmed that 5.8 μM 2′-d-3′-GMP of the 370 μM 2′-d-3′-GMP included binds to the 17.5 μM ferrous enzyme at 15 °C in the absence of CO (data not shown). The midpoint

dx.doi.org/10.1021/bi3004044 | *Biochemistry* 2012, 51, 9277–9289

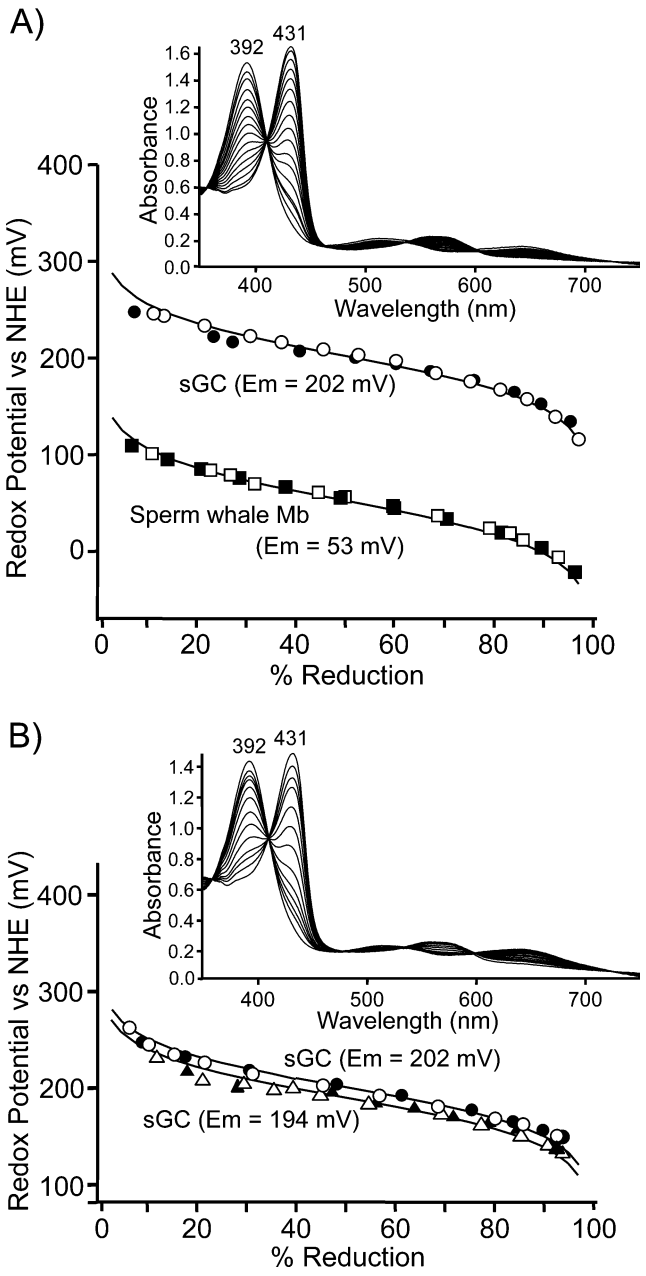

Figure 8. Anaerobic spectroelectrochemical redox potential titrations at 15 °C. The reaction mixture was composed of approximately 15 μM myoglobin or sGC in 50 mM Hepes buffer (pH 7.5) containing 0.1 M KCl and 5% glycerol. (A) Data points for myoglobin and sGC obtained by spectroelectrochemical titrations are indicated by squares , respectively; the empty and filled symbols denote data determined by reductive and oxidative titrations, respectively. (B) Redox potentials of sGC were determined in the presence of 80 μM BAY 41-2272 and 1.5 mM Mg^{2+} (circles) and after the combined addition of 80 μM BAY 41-2272, 500 μM 2′-d-3′-GMP, 500 μM foscarnet, and 1.5 mM Mn^{2+} (triangles). Empty and filled symbols denote midpoint potentials obtained by reductive and oxidative titrations, respectively.

potential measured under the corresponding condition is reduced by only 8 mV (Figure 8B). The small decrease might be attributable to the effect of binding of 2′-d-3′-GMP to the catalytic site in the absence of CO. However, the observed effect of 2′-d-3′-GMP on the midpoint potential of the heme may not result from changes in the Fe−proximal His bond strength, as discussed below.

DISCUSSION

sGC is a crucial cellular receptor for the gaseous signaling agent NO. Under physiological conditions, the function of this enzyme seems to be controlled by a complicated relationship among NO, GTP, and ATP.[13,14,29] For instance, GTP and ATP play critical roles as a switch in the interconversion between a weakly active NO−enzyme complex and a fully active NO−enzyme complex. This mechanism may be involved in two distinct NO/cGMP signaling modes mediated by sGC: tonic and acute NO signal transductions. Although the findings highlighted the crucial function of nucleotides in the regulation of sGC activity, other regulatory functions of the nucleotide were not examined in detail. In this study, we found that 2′-d-3′-GMP potently inhibits the sGC-mediated cGMP production at a low micromolar concentration in the presence of physiological activator NO. Furthermore, the inhibitory action is potentiated by allosteric activators, such as BAY 41-2272, other than gaseous heme-binding activator NO. These inhibitory modes of 2′-d-3′-GMP are unique and clearly distinct from those of other substrate analogues such as AMP-PNP and 2′-dADP.[16] The unique inhibitory actions of 2′-d-3′-GMP are analogous to those of nucleotides termed P-site inhibitors for adenylate cyclase. The result described here is the first identification of a P-site inhibitor for soluble guanylate cyclase. Furthermore, the P-site inhibitor is used as a tool for analyzing the reaction catalyzed by guanylate cyclase, because it has been proposed that the P-site inhibitor exclusively binds to the enzyme−product (PP_i) complex in the transition state.

On the basis of the kinetic data presented in this study, the inhibitory actions of 2′-d-3′-GMP in the absence and presence of the activator(s) are summarized in Figure 9A. In this model, allosteric activator BAY 41-2272 is thought to bind to a pseudosubstrate site that is symmetrically related to the catalytic site.[16,17] As shown, the forms of the enzyme stimulated by gaseous heme binding and allosteric activators are more sensitive to the inhibition by 2′-d-3′-GMP, probably via the increase in the steady state concentration of the enzyme−PP_i complex. For instance, the apparent inhibitory potency of 2′-d-3′-GMP increased approximately 1000-fold upon addition of physiological activator NO: K_i for 2′-d-3′-GMP decreased from 470 to 0.48 μM. The marked decrease in the apparent K_i value was also noted when the enzyme was activated by BAY 41-2272 alone or by both CO and BAY. We initially thought that the binding of 2′-d-3′-GMP is associated with weakening or breaking of the Fe−proximal His105 bond, because GTP, which has a core structure homologous to that of 2′-d-3′-GMP, was reported to stimulate the conversion of the six-coordinate NO−heme complex to the five-coordinate NO−heme complex.[14] This possibility is examined by infrared spectroscopy using the CO−enzyme complex combined with YC-1 or BAY 41-2272 (Figure 4 and Figure S3 of the Supporting Information). Contrary to expectation, the binding of 2′-d-3′-GMP caused no detectable increase in the level of the five-coordinate CO−heme complex.

The effect of 2′-d-3′-GMP on the Fe−His bond was also assessed by redox potential measurements of the heme iron. The midpoint potential of sGC is the highest among those of the protoheme-containing high-spin hemoproteins so far reported.[24] How hemoproteins acquire an appropriate midpoint potential is not well elucidated. However, the redox potential of the heme iron is influenced by the axial coordinating ligands,[30,31] electrostatic stabilization of the heme iron,[32] and heme geometrical changes caused by its interaction with residues.[33,34]

dx.doi.org/10.1021/bi3004044 | *Biochemistry* 2012, 51, 9277−9289

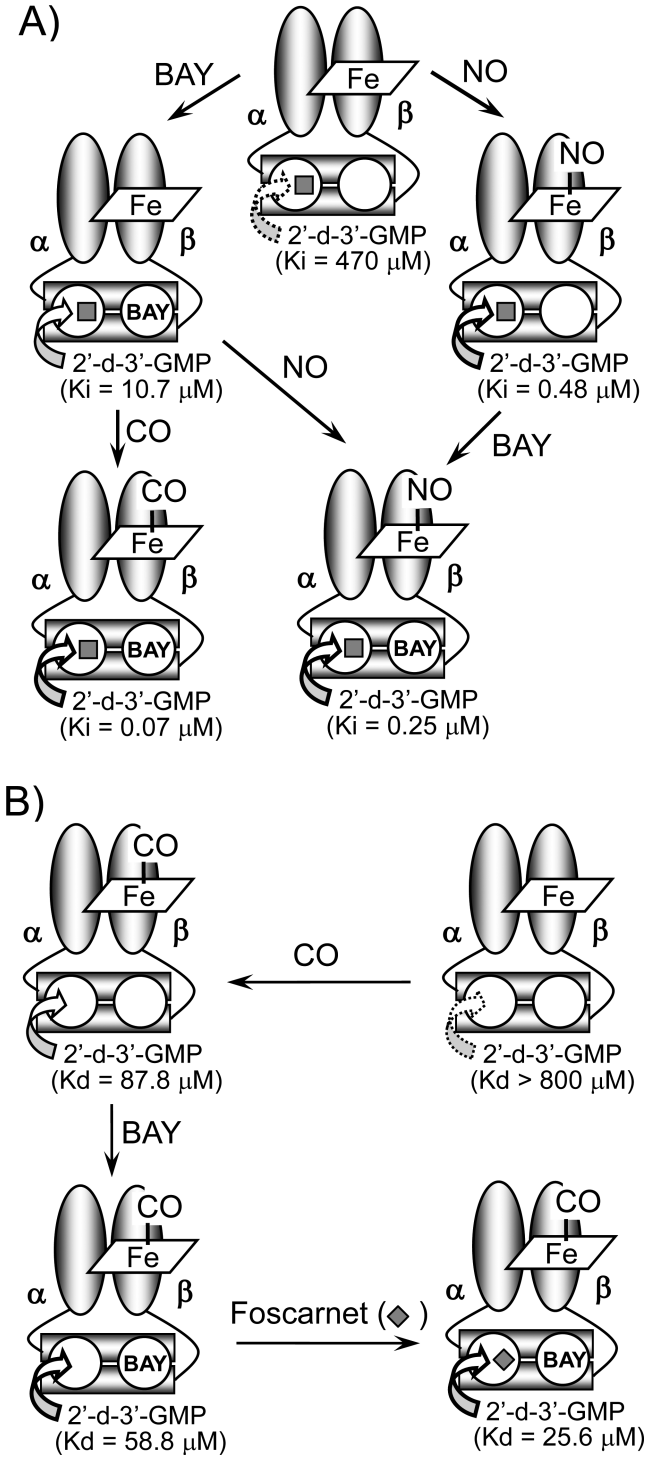

Figure 9. Models proposed for the binding of 2′-d-3′-GMP in the presence of gaseous and allosteric activators. In these figures, apparent inhibition constants (K_i) and dissociation constants (K_d) obtained in the presence of Mn^{2+} are depicted. (A) Effects of CO, NO, and BAY on the inhibitory potency (K_i) of 2′-d-3′-GMP. Each modeled protein species corresponds to the reaction intermediate combined with PP_i. PP_i bound to the enzyme is denoted with a filled square (■). (B) Effects of CO, BAY 41-2272, and foscarnet on the affinity (K_d) of 2′-d-3′-GMP. In this figure, foscarnet is denoted by a diamond (◆). In both models, allosteric activator BAY 41-2272 is thought to bind to a site pseudosymmetric to the catalytic site.[16,17]

Thus, the redox potential is very sensitive to the heme environmental changes. For instance, it is revealed that the binding of an allosteric effector (inositol hexaphosphate) to hemoglobin imposed strain on the Fe−proximal His bond and markedly elevated the midpoint potential of the heme.[30] In this study, the effect of 2′-d-3′-GMP on the redox potential of the heme was examined in the presence of BAY 41-2272, foscarnet, and Mn^{2+}. The results of this experiment revealed that 2′-d-3′-GMP leads to only a small decrease (8 mV) in the measured midpoint potential of the heme. Such a decrease in the midpoint potential may not reflect changes in the strength of the Fe−His bond, because breaking or weakening of the Fe−His bond by imposed strain may result in elevation of the midpoint potential of the heme.[24,30] On the basis of these findings and infrared measurements, we concluded that 2′-d-3′-GMP does not impose severe strain on the Fe−His bond.

The binding of 2′-d-3′-GMP analyzed by equilibrium dialysis is summarized in Figure 9B with the effects of activators. The binding of 2′-d-3′-GMP primarily requires the ligation of CO at the enzymatic ferrous heme. The binding of BAY 41-2272 to a pseudosymmetric site leads to an increase in the affinity of 2′-d-3′-GMP. Foscarnet further increases the affinity of the inhibitor by occupying the catalytic site (Figure 2 and Figure S2 of the Supporting Information). The most striking feature revealed from this study is that 2′-d-3′-GMP is capable of discriminating the minor changes in the conformation of the catalytic site after binding CO. Furthermore, this finding suggests that the CO-enzyme−2′-d-3′-GMP−foscarnet ternary complex mimics a structure of the productlike transition state, accommodating both PP_i and 2′-d-3′-GMP. However, the K_d of 2′-d-3′-GMP for the CO-enzyme−foscarnet complex is ∼25 μM (Figure 2C), which is larger than the apparent K_i value of ∼0.1 μM (Figure 1D) under similar conditions. This discrepancy presumably reflects the structural difference in the catalytic site in the CO-bound enzyme between the resting state and the transition state. Further experiments will be required to analyze these structural changes in detail.

This finding shows that NO seems to synergistically increase the inhibitory potency of 2′-d-3′-GMP when NO binds to the BAY−sGC complex, while BAY 41-2272 does not synergize with the NO−sGC complex (Figure 9A). On the basis of the dead-end inhibition model proposed for adenylate cyclase, the inhibitory potency by a P-site inhibitor depends on the amount of enzyme−PP_i complex that accumulates in the catalytic reaction. Consequently, if the binding of NO to the heme yields a larger amount of the enzyme−PP_i complex than binding of BAY alone, the inhibitory potency of 2′-d-3′-GMP may be primarily dominated by NO, rather than BAY 41-2272. This may account for the reason why NO synergizes with the BAY-bound enzyme to increase the inhibitory potency of 2′-d-3′-GMP, but BAY does not synergize with the NO−sGC complex. Thus, it is feasible that the production of a different amount of the enzyme−PP_i complex by an activator leads to the different degree of apparent synergy for P-site inhibition. The question of why gaseous and allosteric activators exhibit similar potency for 2′-d-3′-GMP inhibition arises, irrespective of their binding at distinct sites. The issue may be explained in terms of domain interaction. Our equilibrium dialysis studies using 2′-d-3′-GMP as the substrate analogue directly demonstrated communication between the heme site and the catalytic site (Figure 2). A recent publication using chimeric sGC proteins revealed the intramolecular communication between the heme domain and the catalytic domain.[35] This was achieved by constructing chimeras

dx.doi.org/10.1021/bi3004044 | Biochemistry 2012, 51, 9277−9289

in which the heme-binding domain of rat sGC was replaced with that of bacterial or eukaryotic sGC homologues. These results taken together lead to a mechanism in which the heme-binding domain makes contact with the catalytic domains to increase the inhibitory potency of 2′-d-3′-GMP. Moreover, these results demonstrate the communication between the catalytic site and the allosteric activator binding site (Figure 3). This may account for the increased inhibitory potency of 2′-d-3′-GMP by BAY 41-2272. The interactions between these sites were further corroborated by means of infrared spectroscopy using the CO complexes (Figure 4 and Figure S3 of the Supporting Information) and by EPR spectroscopy using the NO complex.[23]

The action of N_3^- as an activator for the ferric enzyme was analyzed by infrared and EPR spectroscopic methods. These results provide supporting evidence that N_3^- activated the ferric enzyme by cleaving the Fe−proximal His105 bond to produce a five-coordinate N_3^--bound heme. The formation of the five-coordinate N_3^--bound heme is specific to sGC among hemoproteins so far reported. In accordance with the effects of gaseous heme-binding ligands on the ferrous sGC, N_3^- potentiated the inhibitory action of 2′-d-3′-GMP. To explore whether five-coordinate N_3^--bound heme was produced following six-coordinate N_3^--bound heme, we analyzed the reaction by stopped-flow rapid scan spectrophotometry (data not shown). For instance, the reaction between ferric sGC (4 μM) and N_3^- (20 mM) followed by a stopped-flow method essentially conformed to a pseudo-first-order reaction and did not show any indications of the formation of six-coordinate N_3^--bound heme. This suggests that the rate of conversion of six-coordinate to five-coordinate N_3^--bound heme is much faster than the rate of formation of the six-coordinate N_3^- complex. Alternatively, it is feasible that N_3^- binds directly to the proximal position of the heme by replacing the proximal His residue. Although the precise mechanism remains unresolved, our results strongly suggested that N_3^- exclusively produces a five-coordinate high-spin heme by breaking the Fe−proximal His105 bond.

To the best of our knowledge, the physiological function of guanine nucleotide 3′-phosphates, including 2′-d-3′-GMP, is not explored in eukaryotic systems. On the other hand, the natural occurrence of guanosine 5′-di- and 5′-triphosphate-3′-diphosphate (ppGpp and pppGpp, respectively) has been reported. These compounds, which were isolated from sporulating bacteria, may be involved in the regulation of development. Analogous adenosine 3′-polyphosphates may naturally occur and are thought to be potent P-site inhibitors for adenylate cyclase.[36] If 2′-d-3′-GMP or guanine nucleotide 3′-polyphosphate is at a micromolar level in mammalian tissues, our results suggest that this class of guanine nucleotide acts as an effective intracellular regulator in NO signaling systems.

■ ASSOCIATED CONTENT

Supporting Information

Kinetic studies of the inhibitory action of 2′-d-3′-GMP using Mg-GTP as a substrate (Figure S1), binding of AMP-PNP to ferrous sGC in the presence and absence of CO (Figure S2), effects of 2′-d-3′-GMP on the C−O stretch in the presence of BAY 41-2272 (Figure S3), kinetic studies of the inhibitory action of 2′-d-3′-GMP on N_3^--activated ferric sGC (Figure S4), spectrophotometric titration of the binding of azide to dibromodeuteroheme-substituted sGC (Figure S5), and effects of nucleotides on optical absorption spectra at 75 K and EPR spectra at 15 K of the ferric enzyme (Figure S6). This material is available free of charge via the Internet at http://pubs.acs.org.

■ AUTHOR INFORMATION

Corresponding Author

*R.M.: telephone, 81-042-747-0658; e-mail, rmakino04@rikkyo.ac.jp or 5540512@rikkyo.ac.jp. Y.S.: telephone, 81-0791-58-2817; e-mail, yshiro@riken.jp.

Funding

This work was supported in part by Grants-in-Aid for Scientific Reserch (C) (R.M.) and the Strategic Research Foundation Grant-Aided Project for Private Universities (S1201003) (R.M.) from the Ministry of Education, Culture, Sports, Science and Technology of Japan.

Notes

The authors declare no competing financial interest.

■ ACKNOWLEDGMENTS

We thank Mieko Taketsugu, Ryuzaburo Narita, Taiki Hamano, and Hiro-o Abe for helpful technical assistance.

■ ABBREVIATIONS

sGC, soluble guanylate cyclase; NO, nitric oxide; CO, carbon monoxide; cGMP, cyclic GMP; 2′-d-3′-GMP, 2′-deoxy-3′-GMP (2′-deoxyguanosine 3′-monophosphate); K_d, dissociation constant; K_i, inhibition constant; DTT, dithiothreitol; HPLC, high-performance liquid chromatography; Hepes, 4-(2-hydroxyethyl)-1-piperazineethanesulfonic acid; DMF, dimethylformamide; TEA, triethanolamine; EPR, electron paramagnetic resonance; PP_i, pyrophosphate; AC, adenylate cyclase; AMP-PNP, adenosine 5′-β,γ-imidotriphosphate; GMP-CPP, α,β-methylene guanosine 5′-triphosphate; GMP-PNP, guanosine 5′-β,γ-imidotriphosphate.

■ REFERENCES

(1) Ignarro, L. J., and Kadowitz, P. J. (1985) The pharmacological and physiological role of cyclic GMP in vascular smooth muscle relaxation. *Annu. Rev. Pharmacol. Toxicol. 25*, 171−191.

(2) Waldman, S. A., and Murad, F. (1987) Cyclic GMP synthesis and function. *Pharmacol. Rev. 39*, 163−196.

(3) Garthwaite, J., Charles, S. L., and Chess-Williams, R. (1988) Endothelium-derived relaxing factor release on activation of NMDA receptors suggests role as intercellular messenger in the brain. *Nature 336*, 385−388.

(4) Bredt, D. S., and Snyder, S. H. (1989) Nitric oxide mediates glutamate-linked enhancement of cGMP levels in the cerebellum. *Proc. Natl. Acad. Sci. U.S.A. 86*, 9030−9033.

(5) Moncada, S., and Higgs, E. A. (1991) Endogenous nitric oxide: Physiology, pathology and clinical relevance. *Eur. J. Clin. Invest. 21*, 361−374.

(6) Kamisaki, Y., Saheki, S., Nakane, M., Palmieri, J. A., Kuno, T., Chang, B. Y., Waldman, S. A., and Murad, F. (1986) Soluble guanylate cyclase from rat lung exists as a heterodimer. *J. Biol. Chem. 261*, 7236−7241.

(7) Stone, J. R., and Marletta, M. A. (1994) Soluble guanylate cyclase from bovine lung: activation with nitric oxide and carbon monoxide and spectral characterization of the ferrous and ferric states. *Biochemistry 33*, 5636−5640.

(8) Wedel, B., Humbert, P., Harteneck, C., Foerster, J., Malkewitz, J., Böhme, E., Schultz, G., and Koesling, D. (1994) Mutation of His-105 in the β1 subunit yields a nitric oxide-insensitive form of soluble guanylyl cyclase. *Proc. Natl. Acad. Sci. U.S.A. 91*, 2592−2596.

(9) Zhao, Y., and Marletta, M. A. (1997) Localization of the heme binding region in soluble guanylate cyclase. *Biochemistry 36*, 15959−15964.

(10) Deinum., G., Stone, J. R., Babcock, G. T., and Marletta, M. A. (1996) Binding of nitric oxide and carbon monoxide to soluble guanylate cyclase as observed with resonance Raman spectroscopy. *Biochemistry 35*, 1540−1547.
(11) Makino, R., Matsuda, H., Obayashi, E., Iizuka, T., Shiro, Y., and Hori, H. (1999) EPR characterization of axial bond in metal center of native and cobalt-substituted guanylate cyclase. *J. Biol. Chem. 274*, 7714−7723.
(12) Gerzer, R., Hofmann, F., and Schultz, G. (1981) Purification of a soluble, sodium-nitroprusside-stimulated guanylate cyclase from bovine lung. *Eur. J. Biochem. 116*, 479−486.
(13) Russwurm, M., and Koesling, D. (2004) NO activation of guanylyl cyclase. *EMBO J. 23*, 4443−4450.
(14) Cary, S. P. L., Winger, J. A., and Marletta, M. A. (2005) Tonic and acute nitric oxide signaling through soluble guanylate cyclase is mediated by nonheme nitric oxide, ATP, and GTP. *Proc. Natl. Acad. Sci. U.S.A. 102*, 13064−13069.
(15) Martin, E., Berka, V., Sharma, I., and Tsai, A.-L. (2012) Mechanism of binding of NO to soluble guanylyl cyclase: Implication for the second binding to the heme proximal site. *Biochemistry 51*, 2737−2746.
(16) Yazawa, Y., Tsuchiya, H., Hori, H., and Makino, R. (2006) Functional characterization of two nucleotide-binding sites in soluble guanylate cyclase. *J. Biol. Chem. 281*, 21763−21770.
(17) Chang, F.-J., Lemme, S., Sun, Q., Sunahara, R. K., and Beuve, A. (2005) Nitric oxide-dependent allosteric inhibitory role of a second nucleotide binding site in soluble guanylyl cyclase. *J. Biol. Chem. 280*, 11513−11519.
(18) Winger, J. A., Derbyshire, E. R., Lamers, M. H., Marletta, M. A., and Kuriyan, J. (2008) The crystal structure of the catalytic domain of a eukaryotic guanylate cyclase. *BMC Struct. Biol. 8*, 42.
(19) Florio, V., and Rose, E. (1983) Regulation of the catalytic component of adenylate cyclase. Potentiative interaction of stimulatory ligands and 2′,5′-dideoxyadenosine. *Mol. Pharmacol. 24*, 195−202.
(20) Dessauer, C. W., and Gilman, A. G. (1997) The catalytic mechanism of mammalian adenylyl cyclase. *J. Biol. Chem. 272*, 27787−27795.
(21) Dessauer, C. W., Tesmer, J. J., Sprang, S. R., and Gilman, A. G. (1999) The interactions of adenylate cyclases with P-site inhibitors. *Trends Pharmacol. Sci. 20*, 205−210.
(22) Tesmer, J. J., Dessauer, C. W., Sunahara, R. K., Murray, L. D., Johnson, R. A., Gilman, A. G., and Sprang, S. R. (2000) Molecular basis for P-site inhibition of adenylyl cyclase. *Biochemistry 39*, 14464−14471.
(23) Makino, R., Obayashi, E., Homma, N., Shiro, Y., and Hori, H. (2003) YC-1 facilitates release of the proximal His residue in the NO and CO complexes of soluble guanylate cyclase. *J. Biol. Chem. 278*, 11130−11137.
(24) Makino, R., Park, S.-Y., Obayashi, E., Iizuka, T., Hori, H., and Shiro, Y. (2011) Oxygen binding and redox properties of the heme in soluble guanylate cyclase: Implications for the mechanism of ligand discrimination. *J. Biol. Chem. 286*, 15678−15687.
(25) Mou, T.-C., Masada, N., Cooper, D. M. F., and Sprang, S. R. (2009) Structural basis for inhibition of mammalian adenylyl cyclase by calcium. *Biochemistry 48*, 3387−3397.
(26) Martin, E., Czarnecki, K., Jayaraman, V., Murad, F., and Kincaid, J. (2005) Resonance Raman and infrared spectroscopic studies of high-output forms of human soluble guanylyl cyclase. *J. Am. Chem. Soc. 127*, 4625−4631.
(27) Alben, J. O., and Fager, L. Y. (1972) Infrared studies of azide bound to myoglobin and hemoglobin. Temperature dependence of ionicity. *Biochemistry 11*, 842−847.
(28) Fritz, B., Hu, X., Brailey, J. L., Berry, R. E., Walker, F. A., and Montfort, W. R. (2011) Oxidation and loss of heme in soluble guanylyl cyclase from *Manduca sexta*. *Biochemistry 50*, 5813−5815.
(29) Cary, S. P. L., Winger, J. A., Derbyshire, E. R., and Marletta, M. A. (2006) Nitric oxide signaling: no longer simply on or off. *Trends Biochem. Sci. 31*, 231−239.
(30) Faulkner, K. M., Bonaventure, C., and Crumbliss, A. L. (1995) A spectroelectrochemical method for differentiation of steric and electronic effects in hemoglobins and myoglobins. *J. Biol. Chem. 270*, 13604−13612.
(31) Adachi, S., Nagano, S., Ishimori, K., Watanabe, Y., Morishima, I., Egawa, T., Kitagawa, T., and Makino, R. (1993) Roles of proximal ligand in heme proteins: Replacement of proximal histidine of human myoglobin with cysteine and tyrosine by site-directed mutagenesis as models for P-450, chloroperoxidase, and catalase. *Biochemistry 32*, 241−252.
(32) Gunner, M. R., and Honig, B. (1991) Electrostatic control of midpoint potentials in the cytochrome subunit of the *Rhodopseudomonas viridis* reaction center. *Proc. Natl. Acad. Sci. U.S.A. 88*, 9151−9155.
(33) Olea, C., Kuriyan, J., and Marletta, M. A. (2010) Modulating heme redox potential through protein-induced porphyrin distortion. *J. Am. Chem. Soc. 132*, 12794−12795.
(34) Olea, C., Boon, E. M., Pellicena, P., Kuriyan, J., and Marletta, M. A. (2008) Probing the function of heme distortion in the H-NOX family. *ACS Chem. Biol. 3*, 703−710.
(35) Derbyshire, E. R., Winter, M. B., Ibrahim, M., Deng, S., Spiro, T. G., and Marletta, M. A. (2011) Probing domain interactions in soluble guanylate cyclase. *Biochemistry 50*, 4281−4290.
(36) Desaurby, L., Shoshani, I., and Johnson, R. A. (1966) Inhibition of adenylyl cyclase by a family of newly synthesized adenine nucleotide 3′-polyphophates. *J. Biol. Chem. 271*, 14028−14034.